Proceedings of the ASME 2011 9th Fuel Cell Science, Engineering and Technology Conference
FuelCell2011
August 7-10, 2011, Washington, DC, USA

FuelCell2011-54344

MULTIPLE DEGRADATION PHENOMENA IN POLYMER ELECTROLYTE FUEL CELL OPERATION WITH DEAD-ENDED ANODE

Toyoaki Matsuura[a]*, Jason B. Siegel, Jixin Chen, Anna G. Stefanopoulou

University of Michigan department of Mechanical Engineering, Ann Arbor, Michigan 48109
Email: mtoyo@umich.edu[a]

ABSTRACT

Dead-ended anode (DEA) operation of Polymer Electrolyte Fuel Cell (PEFC) can simplify the fuel cell auxiliary and reduce system cost, however durability and lifetime in this operating mode requires further study. In this work, we investigate the electrode and membrane degradations of one 50 cm^2 active area fuel cell under DEA operation using a combination of post-mortem evaluation and in-situ performance evaluation protocol. We experimentally identify multiple degradation patterns using a cell which we have previously modeled and experimentally verified the spatio-temporal patterns associated with the anode water flooding and nitrogen blanketing. The change in cell voltage and internal resistance during operation and ex situ Scanning Electron Microscope (SEM) images of aged electrode/membrane are analysed to determine and characterize the degradation of the membrane electrode assembly (MEA). Chemical degradations including carbon corrosion in the catalyst layer and membrane decomposition are found after operating the cell with a DEA. Mechanical degradations including membrane delamination are also observed. Unique features of DEA operation including fuel starvation/nitrogen blanketing in the anode and uneven local water/current distribution, are considered as culprits for degradation.

INTRODUCTION

Polymer electrolyte fuel cell (PEFC) is a promising power source for portable or mobile applications, although there are still unresolved issues such as on-board hydrogen storage [1, 2] and effective water management [3,4]. Dead-ended anode(DEA) operation of PEFC [5, 6] simplifies the system by removing the hydrogen recirculation and anode humidification parts. The cost and weight reduction associated with this system simplification is attractive for portable applications. The hydrogen depletion in the anode due to nitrogen blanketing and water flooding results in cell voltage decay with time, therefore periodic purging to remove nitrogen/water and recover voltage is necessary in DEA operation. DEA operation features high spatiotemporal variation of local fuel/water amount and current distribution, which potentially accelerates three major types of degradations in fuel cells, i.e., carbon corrosion in the catalyst layer, membrane polymer decomposition and mechanical degradation of membrane including tear, perforation and delamination.

Carbon corrosion in the catalyst layer of PEFC is caused by elevated interfacial potential (>0.8 V) between the membrane phase and the metal phase which promotes the $C + H_2O \rightarrow CO_2 + H^+ + e^-$ reaction. This elevated potential is usually attributed to the development of a H_2/O_2 boundary during startup/shutdown of the cell [7, 8]. During flow through (FT) fuel cell operating conditions the potential is low and carbon corrosion is negligible. In DEA operation however, the variation of membrane phase potential associated with local fuel depletion can cause increased interfacial potential and carbon oxidization rate. Hence the carbon corrosion, particularly in the cathode, is one phenomenon investigated in this work.

The membrane is vulnerable to both chemical and mechanical degradations during fuel cell operation. The chemical degra-

*

dation generally refers to the hydroxyl radical attack of the perfluorosulfonic acid (PFSA) polymer backbone [9, 10], with the fluoride in the backbone being consumed to generate hydrofluoride. Such degradation may be more severe under high temperature and low RH [11–13]. Furthermore, when PEFC operates under dry/wet or freeze/thaw cycles, the induced mechanical stress normally is detrimental to the membrane durability [14, 15]. Also, the membrane areas corresponding to the land/channel edge and sealing edge are subject to additional stress and therefore small tears or perforation [16]. The membrane delamination with Pt/C catalyst layer may be one of the consequences from stress cycling [17]. Finally, uneven local current distribution may lead to pin-hole failure of the membrane [18], which dramatically increases the fuel crossover rate. The DEA operation features high spatiotemporal variation of local water amount and current, and the cell might experience both chemical and mechanical accelerated degradations over time.

The DEA operation of PEFC is beneficial, but the degradation may be more severe than flow through operation. As reviewed by Wang et al. [19], life time of 5000 hours is desired for fuel cell vehicle applications. Hence, we examine the multiple degradation phenomena in order to develop corresponding control strategies to alleviate these undesired degradations. In this paper, we report and analyse the experimental observations of the degradation phenomena and associated cell performance decays in DEA operation, which is the first step to proposing alleviating strategies.

EXPERIMENTAL

MEA AND SINGLE CELL PREPARATION

A single cell with 50 cm^2 active area is used in this work, the Gas Diffusion Layer (GDL) being the 235 μm thickness carbon paper with Micro Porous Layer (MPL) (SIGRACET GDL 25BC, SGL). The Catalyst Coated Membrane (CCM, Ion Power) is 25 μm thickness electrolyte membrane (Nafion, Dupont) with 0.3 mg cm^{-2} Pt loading on both sides. The CCM and GDL are assembled with endplates to build to single cell.

Twenty five parallel straight channels with 7.3 cm length, 1.78 mm depth and 2.08 mm width are used in the anode, and five parallel semi-serpentine channels with 0.69 mm width and 0.99 mm depth in the cathode. A 45 W heater is attached to the end plates to achieve the desired cell temperature.

EXPERIMENTAL SETUP

Fig. 1 shows the schematic of the experimental setup. The air passes through a bubbler type humidifier before feeding into the cell. There are two supply lines for anode. One is for flow through and another for DEA operation. H_2 is humidified for flow through whereas dry gas is supplied directly for DEA operations. The H_2 supply is controlled by Mass Flow Controller (MFC) for FT, however in DEA operations it is controlled by pressure regulator.

The cell is disassembled to observe aged MEA morphology using Scanning Electron Microscopy (SEM, XL30 ESEM, Philips) technique when substantial performance degradation has been observed. To be specific, that is when the cell voltage hit the low limit of test system, triggering system shutdown as the load increased to 0.4 A cm^{-2} (refer to the discussion of Fig. 6 and Fig. 5). To prepare the samples for SEM diagnosis, the aged MEA is cut into 81 sections as shown in Fig.1. This is a natural division due to the cathode 9-channel design with 9-pass semi-serpentine (5 parallel) geometry. The grey sections indicate the samples for diagnosis. These samples, numbered 1 to 5 from inlet to outlet, are embedded in Epoxy Polymer to observe the cross section of the MEA.

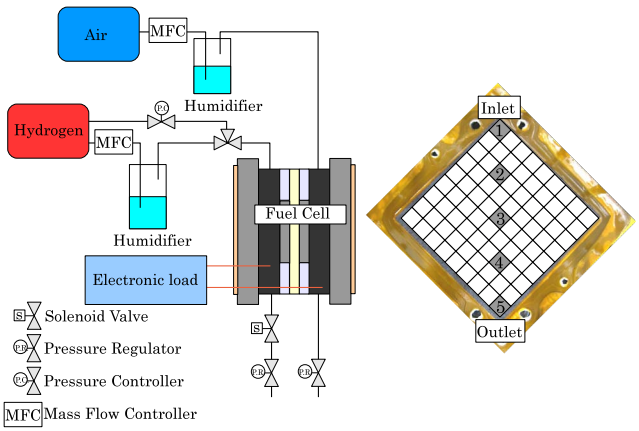

FIGURE 1. Schematic of the fuel cell system and locations of MEA samples.

TYPICAL DEA BEHAVIOR

In Fig. 2, typical voltage drop/recovery behaviors during DEA operation are shown. Crossover nitrogen and water from the cathode accumulate in the anode during DEA operation, which causes gradual voltage drop over time [5, 6, 20]. A scheduled purge which lasts for 0.1 s after 20 minute DEA operation recovers the cell voltage dramatically. In this work, the period from one purge event to the next one is defined as a cycle. During that cycle the voltage decay rate (see Fig.2) is defined as dV/dt. Also, the cell voltage right before purge is defined as V_{bp} and after purge as V_{ap}.

Note that a model of the spatio-temporal patterns during DEA operation for this specific cell has been developed in [6,20] and validated using neutron imaging and simultaneous gas chromatography measurement at the the National Institute of Stan-

dards and Technology (NIST), Center of Neutron Research [6]. Future publication will link the experimental observations from this paper with the model predictions for the expected degradation.

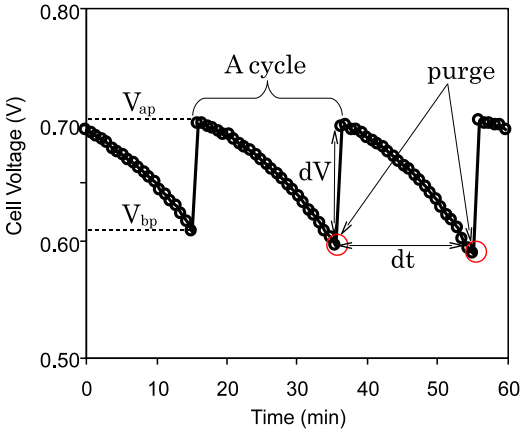

FIGURE 2. Typical voltage behavior during DEA.

DETAILS OF EXPERIMENT

The aged cell before SEM diagnosis has run for 196 hours in total. The details of life-time operation are summarized in Table 1. The cell was at first running 10 hours for conditioning the membrane (Pre-NIST). In the next 120 hours, the cell was running under neutron imaging at NIST [6]. The Pre-Deg in Table 1 indicates the initial performance evaluation before starting the degradation test, which is the same with the evaluation protocol shown in the flow chart of Fig. 3. The purge in the DEA operation is triggered when 20 minutes have elapsed or the cell voltage reduces to 0.4 V, whichever occurs earlier. It is also worthy to mention that the anode gas supply is dry without humidification in DEA operation whereas fully humidified gas is used for FT operationin FT. The relevant operating conditions are detailed in Table 1 and Fig. 3. To prevent additional degradation that may occur during shutdown and start-up [8], the cell was purged with nitrogen until the cell voltage reduced to 0.65 V at the end of each test day before system shutdown.

RESULTS AND DISCUSSION

PERFORMANCE DECAY

Fig. 4 shows the time for each current load under which the cell was running with either DEA or FT operation. Totally the

Period	**Mode**	$\mathbf{T}_{cell}$ ^{o}C	$\mathbf{T}_{Rxt}$ ^{o}C	$\mathbf{SR}_{AN}$	$\mathbf{SR}_{CA}$	**I** A cm^{-2}
Pre-NIST	FT	45-65	45-60	1.2	1.5/2.5/3.0	0-0.8
NIST [6]	DEA	55-70	55-70	1.0	2.0/3.0	0-0.8
	FT	45-70	45-75	1.2	2.5	0-0.8
Pre-Deg	FT	45-65	45-65	1.2	1.5/2.5/3.0	0-0.8
Degd Test (AN/CA)	DEA	60	- /60	1.0	2.5	0-0.8
	FT	60	50/60	1.2	2.5	0-0.8

TABLE 1. Life time operation log of the cell. The events are listed chronologically. After these events, the cell was disassembled for MEA diagnosis. The system pressure is kept at 4.0 psig for all operations. The controlled temperatures for both reactants (T_{Rxt}) are the same. In DEA operation, the anode supply is fully dry without humidification whereas the cathode is fully humidified.FT (flow through), SR (stoichiometry ratio).

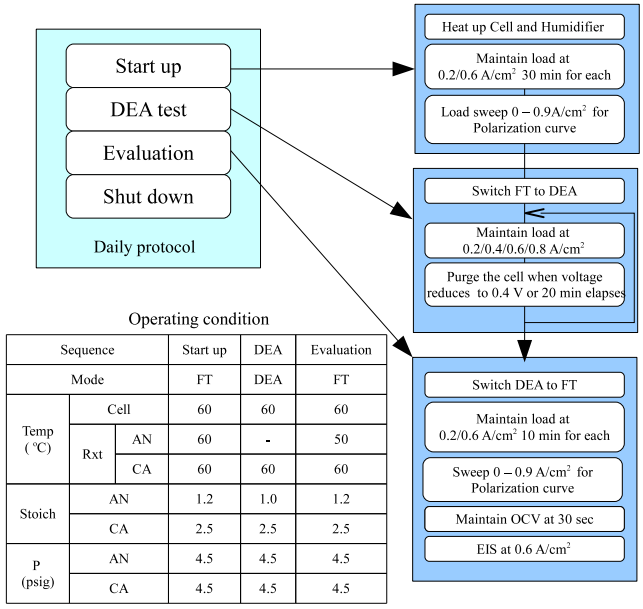

FIGURE 3. Daily performance evaluation protocol during the degradation test. In DEA operation, the anode supply is fully dry without humidification whereas cathode is fully humidified.

cell has run 196 hours. During the DEA operation, the cell operates at 0.2, 0.4, 0.6 and 0.8 A cm^{-2} loads. During other time (performance evaluation), the cell runs FT.

In Fig. 5, the complete voltage response during the whole degradation test are presented with detailed operating conditions in the upper subplots. The vertical lines indicate the switch between degradation test (DEA) and performance evaluation (FT). The third subplot shows the RH profile, with occasional over-

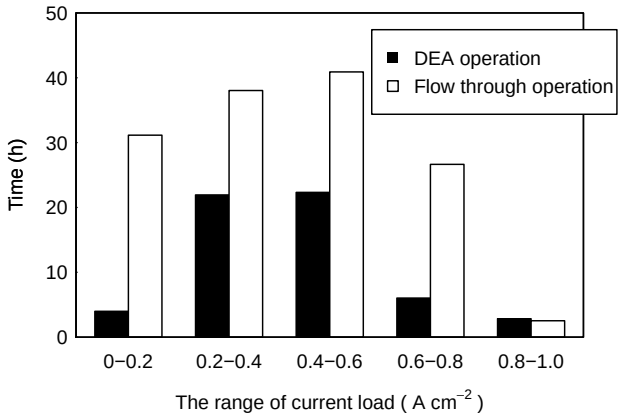

FIGURE 4. Distribution of time at each load currents for DEA, and FT operation.

saturation (RH higher than 100 %) observed. This is because after start-up, the cell temperature may be lower than the dew point of the incoming reactants as it is being heated. Thus, oversaturation occurs only at the beginning of each start up, which has little influence on the whole degradation test. The cell voltage experiences obvious drop after 3000 min although the load is reduced to 0.4 A cm^{-2} (see Fig. 6). This is an indication of combined degradation effects. The erratic surges of cell voltage after 3800 minutes are the result of attempts to determine pin-holes in the membrane via OCV evaluation.

Figure 6 reports the historical profile of current load during the complete degradation test. As can be seen, the cell operates under 0.4 and 0.8 A cm^{-2} loads during most of the degradation test. When the load switches back to 0.4 A cm^{-2} after running under 0.8 A cm^{-2} for 40 cycles and 0.6 A cm^{-2} for 20 cycles, the voltage decays rapidly (see Fig. 8) within a few minutes, indicating serious degradation of the MEA. The degradation test was therefore terminated for SEM diagnosis.

Figure 7 shows the evaluation of dynamic polarization curve and back pressure at selected times (see Fig. 5). The setpoints of current were scanned at a rate of 0.5 A s^{-1} to obtain these dynamic polarization curves. No performance loss can be observed from the polarization curve.

Figure 8 presents the evolution of cell voltage in selected cycles of the degradation test, with the current load being 0.4 A cm^{-2}. Each curve corresponds to the marked evaluation event with the same marker in Fig. 6. In the case of the 8th cycle, the cell voltage decreases for 100 mV during the whole cycle. Similar decrease can be observed in the case of 85th cycle. Finally at the 174th cycle, the cell voltage decreases more than 300 mV within a few minutes. This rapid decay suggests that some significant failure has occurred between the 85th and 174th cycle. It is found that the membrane malfunctioned shortly before the 174th cycle due to pin-hole and/or delamination. During DEA

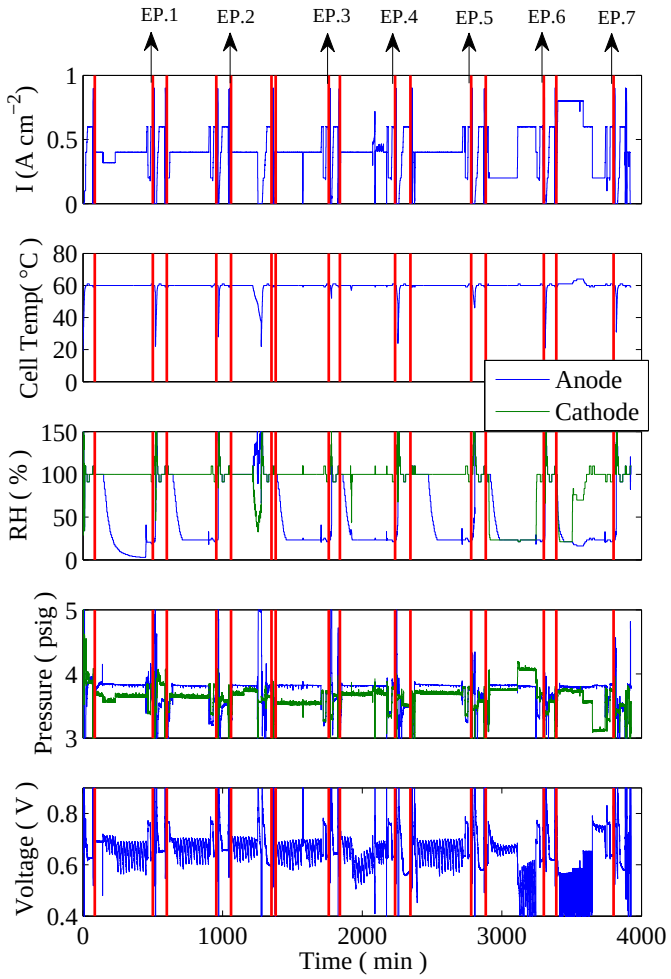

FIGURE 5. Cell voltage profile with operating conditions (current density, cell temperature, RH of air supply and system pressure) during the whole degradation test. EP is short-handed for evaluation point at which the polarization curves in Fig. 7 are obtained.

operation, the pressure difference was set much higher than FT operation (Fig. 5). More hydrogen will be pushed through pass the membrane compared with the FT case due to the higher pressure difference when a pin hole failure occurs in the membrane. Hence, the pin hole failure had a larger impact on cell voltage for DEA operation as compared to FT operation.

Figure 9 presents the voltage decay rate, after-purge voltage, OCV and high frequency resistance in each cycle of the degradation test. During 0.4 A cm^{-2} load periods, which corresponds to 8th-85th cycles in Fig. 6. The rate of voltage decay was around 5 mV sec^{-1} during that period, indicating that the cell has not experienced significant degradation. Focusing on the 0.8 A cm^{-2}

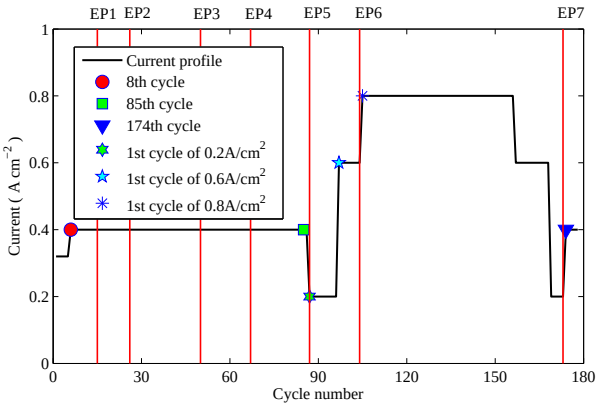

FIGURE 6. Historical profile of current load during degradation test. The marked events correspond to the curves in Fig. 8 and Fig. 15 using the same markers.

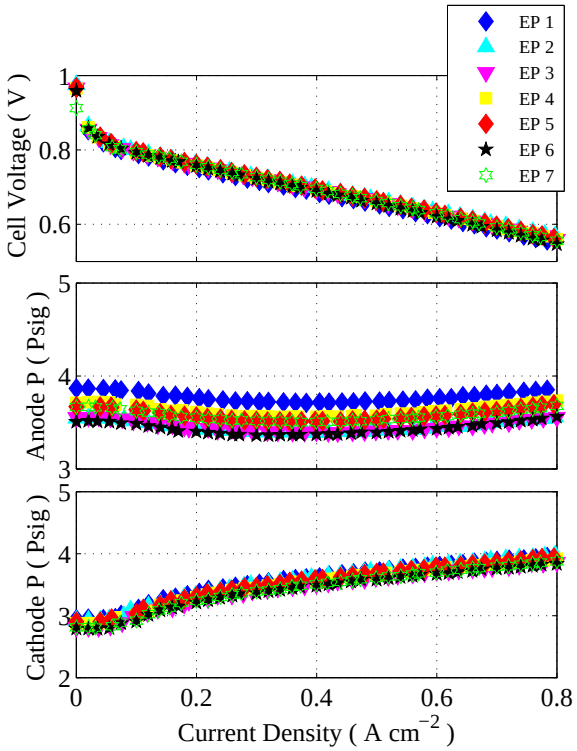

FIGURE 7. The evolution of dynamic polarization with time.The cathode pressure increases with current density due to increased gas flow rate with constant SR operation.

load period corresponding to the 105th-156th cycles in Fig. 6,

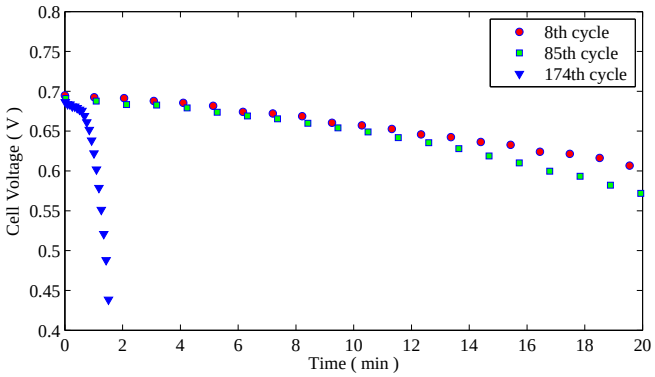

FIGURE 8. Voltage evolution in a DEA operation cycle under 0.4A cm^{-2} load, each curve corresponds to the marked event with the same marker in Fig. 6.

one can observe that the initial rate of voltage decrease is ~20 mV/sec. The rate is then increasing cycle by cycle, finally doubles at the end of 0.8 A cm^{-2} load period. These results indicate that the cell degradation accelerates during 0.8 A cm^{-2} load period.

V_{ap} is related to the applied current load, and highly influenced by the remaining liquid water/nitrogen amount in the anode after purge. Examining the V_{ap} level when the load is 0.4 A cm^{-2} (before and after elevated load of 0.8 A cm^{-2}), we observe slight drop, which might be also a sign of MEA degradation.

The lower subplot of Fig. 9 shows the measurement of OCV at the end of each day. OCV is maintained over 0.95 V before 0.8 A cm^{-2} cycles, after which it reduces to 0.92 V at ~170th cycle. It is usually considered that decrease of OCV can be attributed to the membrane pin-hole and associated high hydrogen crossover [11, 12, 21, 22]. Therefore, membrane pin-hole failure may take place during the elevated load of 0.8 A cm^{-2}, after which the consequence of uneven local current distribution becomes most detrimental. It is interesting to note that the HFR remains fairly low and stable during the degradation test, except for the 0.8 A cm^{-2} load period in which slight increase of HFR is observed. Since HFR is an indicator of the contact resistance of MEA components with end plates, the cell can be considered well-assembled and compressed. The additional amount of water during 0.8 A cm^{-2} operation may contribute to the slight HFR increase.

SEM DIAGNOSIS

In this section we present the SEM images after the aged cell has been disassembled. Fig. 10 presents the SEM images from locations No.1 to No.5 as indicated in Fig. 1. The membrane thickness at location No.1 is clearly thinner than other locations. The sample variance is shown in Fig. 11 using error bars for the whole length of samples (1cm). The membrane thickness from locations No.2 to No.5 ranges from 25μm to 30μm whereas the

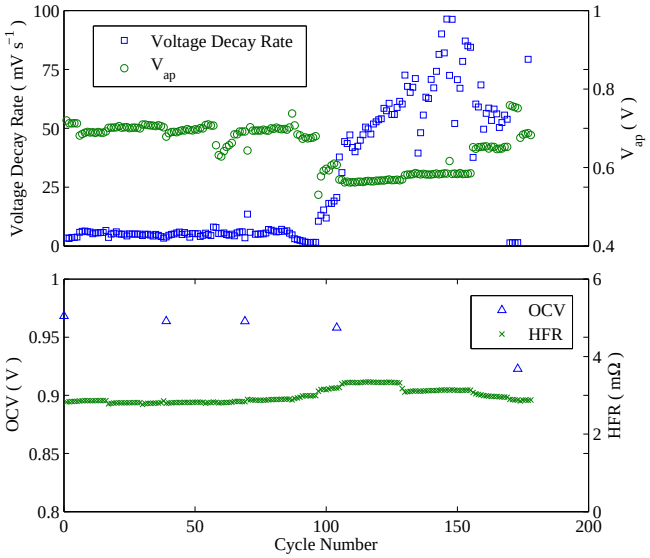

FIGURE 9. Combined plots of voltage decay rate, after-purge voltage, OCV and high frequency resistance during the degradation test.

membrane thickness at location No.1 (inlet) is around 10 μm. The original thickness of the fresh membrane is 30 μm. Thinning of the membrane may be attributed to local polymer decomposition. It has been reported that the membrane decomposition proceeds more rapidly under low RH [9, 10], which is consistent with our observations since the membrane is much drier at the inlet. Note that in DEA operation the liquid water accumulates from the channel end towards the inlet whereas the fully dry hydrogen supply becomes humidified via an opposite direction. The membrane decomposition in specific location also confirms the uneven local water/current distribution in the DEA operation observed during neutron imaging of the fuel cell [5].

Fig. 12 is a bar plot showing the thickness of anode catalyst layer sample, with the original thickness being 15 μm. As can be seen, the thickness of anode catalyst layer is almost unchanged from inlet to outlet. Modeling studies from [7,8] already indicate that the carbon corrosion at the anode is negligible compared with cathode, due to the much smaller interfacial potential between the anode metal phase and membrane phase compared with cathode. It is thus expected that the local fuel starvation and oxygen presence in the anode channel, unique features in the DEA operation, produces negligible impacts on the anode C/Pt electrode. However, the thickness distribution of cathode catalyst layers shown in Fig.13 indicates that the difference from inlet to outlet is ~30%, as well as substantial thinning at location 5 (original thickness 13 μm). At the outlet region of cathode where the most severe local fuel starvation occurs in the anode, the carbon corrosion and resulting electrode thinning is most severe. This

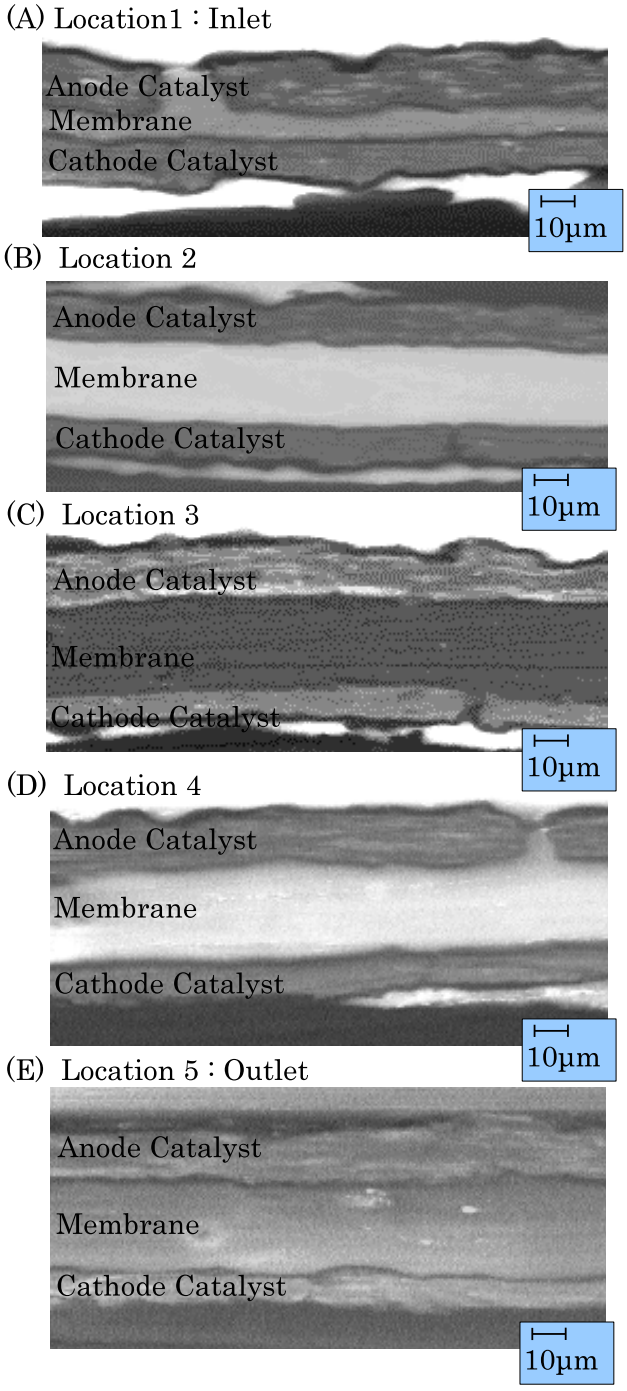

FIGURE 10. SEM images from locations 1 to 5.

observation is consistent with the results in [23].

One more interesting degradation phenomenon, membrane delamination, is observed at the inlet region. Fig. 14 shows a snapshot of the SEM image also taken at location 1, in which

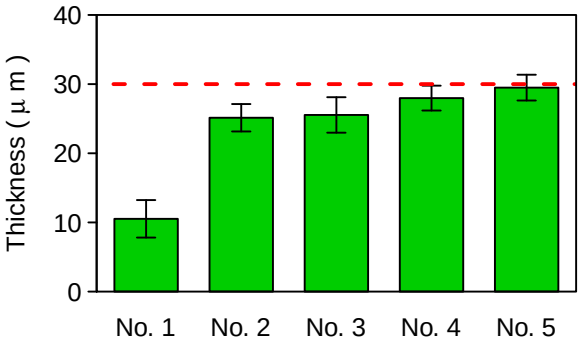

FIGURE 11. The membrane thickness average at each location. The error bars indicate the data range of 300 different points at the sample. The dotted red line indicates the original thickness when the MEA was fresh. The meanings of error bar and dotted red line are the same in Fig. 12 and Fig. 13.

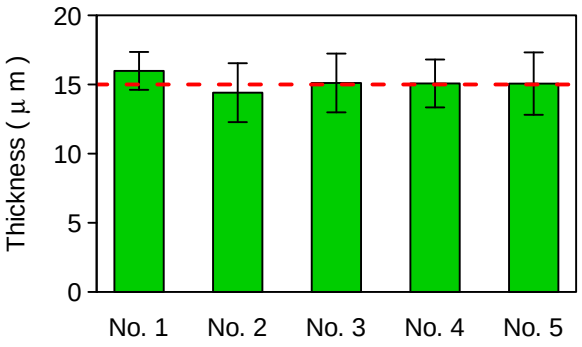

FIGURE 12. The thickness of anode catalyst layer.

we suspect an observation of membrane delamination. The membrane becomes disconnected in the through-plane direction, which might be attributed to the excessive stress close to the sealing gasket under frequent dry/wet cycles of the whole membrane. The membrane fabrication process may be related to this phenomenon. For example, if the Nafion membrane is fabricated from two sandwiched layers of Nafion film, such delamination is very likely to occur. Catalyst layer/membrane delamination is also observed at some spots. Such degradation may be associated with the mechanical stress induced degradation [14, 24] and uneven current distribution.

Fig. 15 shows the voltage and internal resistance evolution within a cycle for different loads. Internal resistance is increasing

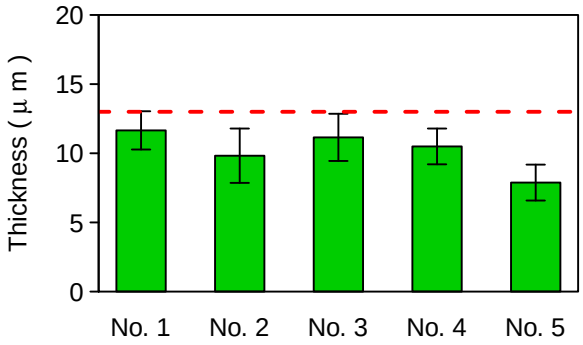

FIGURE 13. The thickness of cathode catalyst layer.

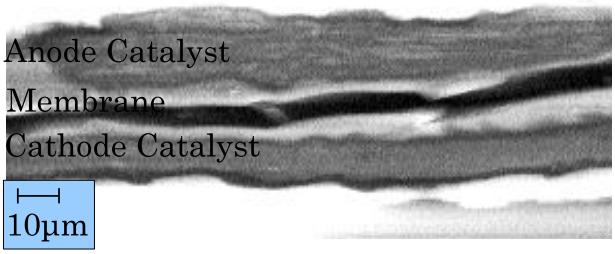

FIGURE 14. SEM image from location 1 showing clear membrane self-delamination.

at 0.001 mΩ min^{-1} when the cell is applied 0.4A cm^{-2} load, whereas at 0.025 mΩ min^{-1} when applied 0.8A cm^{-2} load.

The increase of the internal resistance indicates the drying of the membrane because membrane dehydration results in decrease of ion conductivity [15, 25]. It is expected that the membrane dehydration proceeds more rapidly at elevated loads due to electro-osmotic drag. The elevated load also deteriorates membrane pin-hole failure and increases the hydrogen crossover rate, which may explain the observed high rate of voltage drop in Fig. 9.

Conclusions

It is found that there are three major degradation patterns associated with DEA operations. Carbon corrosion in the catalyst layer is observed substantially at the cathode outlet, whereas the membrane polymer decomposition/delamination is observed near the inlet. Degradation phenomena observed in this work was not observed for the whole anode catalyst layer or the away from the inlet. The amount of carbon corrosion and polymer de-

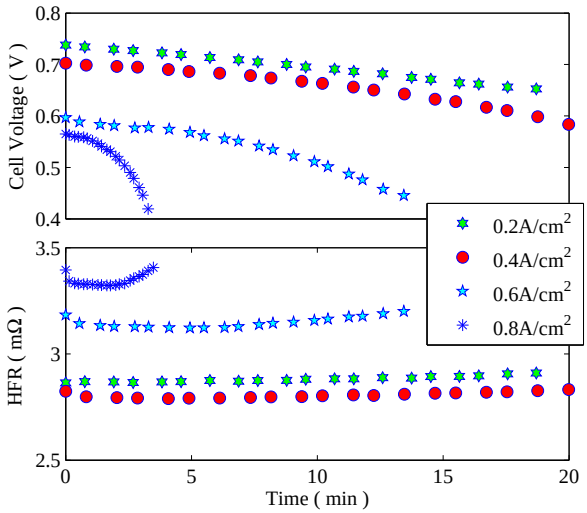

FIGURE 15. Voltage and internal resistance behaviors under different loads in degradation test. Each curve corresponds to the marked event with the same marker in Fig. 6.

composition do not influence the cell performance significantly in FT operation because the reactants are still separated and there is sufficient remaining catalyst to support the reaction. However, the pin-hole failure of membrane clearly affect to cell performance in DEA operation because hydrogen crossover from anode to cathode could increase dramatically due to high pressure difference. These facts suggest that MEA is normally aged slowly even in DEA operation, however, sudden acceleration may occur after pin-hole failure. The degradation is much more severe under high current loads, which produces more uneven water/current distribution and higher membrane dehydration in the inlet region. The delamination of Nafion films is also observed, which may be related to the fabrication process. The collected experimental data can be utilized in the future to tune related degradation models for DEA operations. These models will then be used for a plate-to-plate cell design specifically tailored to mitigate the DEA degradation, increase endurance, hence making the DEA mode competitive to the more traditional flow through operation.

ACKNOWLEDGMENT

This work is funded by the National Science Foundation through CBET-0932509 and Ford Motor Company.

REFERENCES

[1] Chalk, S., and Miller, J., 2006. "Key challenges and recent progress in batteries, fuel cells, and hydrogen storagenext term for clean energy systems". *Journal of Power Sources,* ***159***, pp. 73–80.

[2] Wang, Y., Adroher, X., Chen, J., Yang, X., and Miller, T., 2009. "Three-dimensional modeling of hydrogen sorption in metal hydride hydrogen storage beds". *Journal of Power Sources,* ***194***(2), pp. 997–1006.

[3] Wang, Z., Wang, C.-Y., and Chen, K., 2001. "Two-phase flow and transport in the air cathode of proton exchange membrane fuel cells". *Journal of Power Sources,* ***94***, pp. 40–50.

[4] Chen, J., and Zhou, B., 2008. "Diagnosis of PEM fuel cell stack dynamic behaviors". *Journal of Power Sources,* ***177***, pp. 83–95.

[5] Siegel, J., McKay, D., Stefanopoulou, A., Hussey, D., and Jacobson, D., 2008. "Measurement of liquid water accumulation in a PEMFC with dead-ended anode". *Journal of the Electrochemical Society,* ***155***, p. B1168.

[6] Siegel, J., Bohac, S., Stefanopoulou, A., and Yesilyurt, S., 2010. "Nitrogen front evolution in purged polymer electrolyte membrane fuel cell with dead-ended anode". *Journal of The Electrochemical Society,* ***157***, p. B1081.

[7] Meyers, J., and Darling, R., 2006. "Model of carbon corrosion in PEM fuel cells". *Journal of Electrochemical Society,* ***153***, pp. A1432–A1442.

[8] Reiser, C., Bregoli, L., Patterson, T., Yi, J., Yang, J., Perry, M., and Jarvi, T., 2005. "A reverse-current decay mechanism for fuel cells". *Electrochemical Solid-State Letters,* ***8***, pp. A273–A276.

[9] Curtin, D., Lousenberg, R., Henry, T., Tangeman, P., and Tisack, M., 2004. "Advanced materials for improved PEMFC performance and life". *Journal of Power Sources,* ***131***, pp. 41–48.

[10] Mittal, V., Kunz, H., and Fenton, J., 2007. "Membrane degradation mechanisms in PEMFCs". *Journal of Electrochemical Society,* ***154***, pp. B652–B656.

[11] Zhang, S., Yuan, X., Hin, J., Wang, H., Wu, J., Friedrich, K., and Schulze, M., 2010. "Effects of open-circuit operation on membrane and catalyst layer degradation in proton exchange membrane fuel cells". *Journal of Power Sources,* ***195***(4), pp. 1142–1148.

[12] Teranishi, K., Kawata, K., Tsushima, S., and Hirai, S., 2006. "Degradation mechanism of PEMFC under open circuit operation". *Electrochemical and Solid-State Letters,* ***9***, p. A475.

[13] Tang, H., Peikang, S., Jiang, S., Wang, F., and Pan, M., 2007. "A degradation study of Nafion proton exchange membrane of PEM fuel cells". *Journal of Power Sources,* ***170***(1), pp. 85–92.

[14] Kang, J., and Kim, J., 2010. "Membrane electrode assembly degradation by dry/wet gas on a PEM fuel cell". *International Journal of Hydrogen Energy,* ***35***, pp. 13125–13130.

[15] Baumgartner, W., Parz, P., Fraser, S., Wallnofer, E., and Hacker, V., 2008. "Polarization study of a PEMFC with four reference electrodes at hydrogen starvation conditions". *Journal of Power Sources,* ***182***(2), pp. 413–421.

[16] Wu, J., Yuan, X., Martin, J., Wang, H., Zhang, J., Shen, J., Wu, S., and Merida, W., 2008. "A review of PEM fuel cell durability:degradationnext term mechanisms and mitigation strategies". *Journal of Power Sources,* ***184***, pp. 104–119.

[17] Rong, F., C, H., Liu, Z.-S., and D. Song, Q. W., 2008. "Microstructure changes in the catalyst layers of pem fuel cells induced by load cycling Part I. Mechanical model". *Journal of Power Sources,* ***175***, pp. 699–711.

[18] Weber, A., 2008. "Gas-crossover and membrane-pinhole effects in polymer-electrolyte fuel cells". *Journal of Electrochemical Society,* ***155***, pp. B521–B531.

[19] Wang, Y., Chen, K., Mishler, J., Cho, S., and Adroher, X., 2011. "A review of polymer electrolyte membrane fuel cells: Technology, applications, and needs on fundamental research". *Applied Energy,* ***88***, pp. 981–1007.

[20] Siegel, J., Stefanopoulou, A., Ripaccioli, G., and Di Cairano, S., 2010. "Purge Scheduling for Dead-Ended Anode Operation of PEM Fuel Cells," to appear in *The Control Handbook, Second Edition: Control System Applications, Second Edition*. CRC Press.

[21] Zhang, J., Tang, Y., Song, C., Zhang, J., and Wang, H., 2006. "PEM fuel cell open circuit voltage (OCV) in the temperature range of 23 C to 120 C". *Journal of Power Sources,* ***163***(1), pp. 532–537.

[22] Wu, J., Yuan, X., Martin, J., Wang, H., Yang, D., Qiao, J., and Ma, J., 2010. "Proton exchange membrane fuel cell degradation under close to open-circuit conditions:: Part I: In situ diagnosis". *Journal of Power Sources,* ***195***(4), pp. 1171–1176.

[23] Taniguchi, A., Akita, T., Yasuda, K., and Miyazaki, Y., 2004. "Analysis of electrocatalyst degradation in PEMFC caused by cell reversal during fuel starvation". *Journal of Power Sources,* ***130***(1-2), pp. 42–49.

[24] Huang, X., Solasi, R., Zou, Y., Feshler, M., Reifsnider, K., Condit, D., Burlatsky, S., and Madden, T., 2006. "Mechanical endurance of polymer electrolyte membrane and PEM fuel cell durability". *Journal of Polymer Science Part B: Polymer Physics,* ***44***(16), pp. 2346–2357.

[25] Paquin, M., and Fréchette, L., 2008. "Understanding cathode flooding and dry-out for water management in air breathing PEM fuel cells". *Journal of Power Sources,* ***180***(1), pp. 440–451.